Parameterizing the Antarctic stable boundary layer: synthesising models and observations

K. T. Walesby and R. J. Beare*
University of Exeter, UK.
*Correspondence to: Harrison Building, North Park Road, Exeter, Devon, UK, EX4 4QF.

The accurate representation of the stable boundary layer (SBL) is a key issue for weather prediction and climate models. The SBL exerts an important influence in controlling heat, moisture and momentum fluxes between the surface and the rest of the atmosphere. Some of the world's most stably stratified boundary layers develop on the Antarctic continent. Previous work investigating SBLs has tended to take either a purely observational or purely modelling-based approach. Here, a novel three-way methodology has been developed which uses observations from an Antarctic site, alongside large-eddy simulation (LES) and single-column model (SCM) techniques to examine a case study.
Reasonable agreement was generally achieved between the LES and observations. The choice of stability function is an important decision for column-based parameterizations of the SBL. Four schemes were tested in the SCM, providing persuasive evidence for the use of shorter-tailed stability functions. The LES data was also used to extract implied stability functions. These experiments reinforced the conclusion that shorter-tailed stability functions offered improved performance for the Antarctic stable boundary layer. This approach represents a powerful framework for verifying SCM and LES results against a range of in-situ observations.

Key Words: stable boundary layers; turbulence parameterizations; Antarctic boundary layers

Received . . .

1. Introduction

The accurate representation of the stable boundary layer (SBL) is a key issue for weather prediction and climate models. The SBL exerts an important influence in controlling heat, moisture and momentum fluxes between the surface and the rest of the atmosphere. In addition, humans spend almost their entire lives in the boundary layer. Understanding and predicting its characteristics is thus of pervasive importance.

In the mid-latitudes, SBLs typically form during the nighttime, when the properties of the atmospheric boundary layer (ABL) are very different from those which prevail during the day. After sunset, longwave radiation emitted by the ground surface dominates the radiation budget and leads to surface cooling (since most land surfaces have a higher emissivity than air). This results in a corresponding cooling of the overlying air, with near-surface air reaching the lowest temperatures. A temperature inversion forms, which grows upwards from the surface. Since air density decreases with temperature, buoyancy forces inhibit mixing of air parcels under this temperature profile: an air parcel displaced a small distance from its position will tend to return to its initial position. The degree of stratification exerts a strong influence on the extent of turbulent transfer in the ABL. Turbulent transfer and mixing tend to be suppressed in the SBL (Kondo et al. 1978).

Weather and climate models require subgrid-scale parameterization schemes to describe the effect of processes that are unresolved by the model's grid structure. Atmospheric boundary layer turbulence is one such process. The overall skill of the model output is partly dependent on the accuracy of the chosen turbulent parameterization scheme. Furthermore, the faithful representation of the SBL in models is crucial in many of the most important forecasting applications, including minimum temperature forecasting, fog prediction and air-quality modelling. However, the SBL parameterizations used in weather and climate models remain surprisingly simplistic, given the complexities of the turbulence they are attempting to capture. For example, the Met Office Unified Model (MetUM) employs a first-order turbulence closure for the stable boundary layer (Brown et al. 2008). Such a closure scheme employs a stability function that largely encapsulates the effect of turbulence on the flow. Such functions are required to account for the competition between stability and wind shear.

Progress in the study of the SBL has been hampered by a number of challenges. Efforts towards understanding and modelling the SBL are complicated by the wide variety of physical processes that it supports. Firstly, terrain effects are generally more important in the SBL. Even a very slight slope can significantly influence the evolution of such boundary layers, by producing surface-drainage flows (Monti et al. 2002). The SBL is also more sensitive to surface heterogeneity than the convective

boundary layer (CBL). This is because representation errors can become more profound in stable conditions, when observations are more strongly influenced by local characteristics, whilst model grids are more representative of a larger area. Thirdly, since the SBL forms as a consequence of the surface's radiative cooling, the diurnal cycle of this forcing may never permit the SBL to truly reach a steady-state. Fourthly, stable stratification suppresses vertical transfer, and this can result in intermittent turbulence (Van de Wiel et al. 2002). Other complicating issues include clear-air radiative-flux divergence (Garratt and Brost 1981), decoupling (Derbyshire 1999), the formation of low-level jets (Malcher and Kraus 1983) and gravity wave activity (Hooke and Jones 1986).

The parameterization schemes of numerical weather prediction (NWP) and climate models must attempt to reproduce the above processes, along with their interactions. In reality, it is very challenging to correctly describe all of these processes in a numerical model. The possible influence of such mechanisms also complicates the interpretation of results from observational studies, particularly in the very stable boundary layer. Although comparisons between model parameterizations and observations have identified weaknesses in the parameterizations used in NWP models (see Beljaars and Viterbo 1998), a straightforward route towards addressing these discrepancies is rarely obvious.

Recently, more intensive efforts have been directed towards the challenges of successfully modelling the stable boundary layer. Over the past decade, the Global Energy and Water Cycle Experiment (GEWEX) Atmospheric Boundary Layer Study (GABLS) initiative has delivered tangible progress. The overall aim of GABLS is to enhance understanding and to improve representation of boundary-layer processes in weather and climate models (Holtslag 2006). This initiative gave particular attention to the sensitivity of turbulence within the SBL to details in the mixing formulation, and interactions with the land surface. The first effort of the GABLS initiative was known as GABLS-1. This used large-eddy simulations (LES, Beare et al. (2006b)) as a reference for single column model (SCM) simulations (Cuxart et al. 2006). These experiments were based on the idealised Arctic stable boundary layer case described by Kosovic and Curry (2000). Subsequent GABLS studies have focused on capturing the diurnal cycle (Svensson et al. 2011), the low-level jet (Basu et al. 2012) and coupling to the land surface (Bosveld et al. 2014a,b) in the mid-latitudes, and have linked their case studies more closely with observations. Also, Sterk et al. (2015) performed a SCM comparison with observations for several snow-covered sites. These studies have often highlighted the usefulness of both LESs and SCMs for the SBL, and also how challenging initialising and validating simulations of the SBL with observations remains. To date, there has been only limited use of observations to validate the results of LES. GABLS-1, in particular, was only weakly connected with observations (Beare et al. 2006b). There is a pressing need for studies to strongly root LES and SCM experiments in observed case studies.

Some of the world's most stably stratified boundary layers develop on the Antarctic continent. Antarctica has long been recognised as a location which offers a number of advantages for observation-based, boundary layer studies (King et al. 1989). These advantages have resulted in Antarctica being termed "*a natural laboratory for studying the stable boundary layer*" (King and Turner 2007). It is imperative when modelling the response of the high-latitudes to changes in atmospheric forcing to accurately parameterize the heat, momentum and moisture fluxes across the stable boundary layer. It has been demonstrated, however, that the representation of crucial aspects of the Antarctic weather and climate, such as katabatic flows, are very sensitive to SBL formulation in models (King et al. 2001).

This study presents investigations into high-latitude stable boundary layers, using several modelling techniques and *in-situ* observations from an Antarctic research station. As discussed above, there is a real need to use models and observations in concert, rather than taking either a purely observational or model-based approach (e.g. GABLS-1). A core objective of this study will be to more tightly couple boundary layer models with high-quality observations. Section 2 outlines the observational dataset, and numerical models, used in this study. The results obtained using these techniques are presented in Section 3. Finally, these results are discussed further and placed in their wider context in Section 4.

2. Methods

2.1. Overall research strategy

We have argued above that the optimum approach for boundary-layer studies combines a range of numerical modelling techniques with observations. This study adopts just such a strategy. Figure 1 provides a flow diagram of the approach this study used to combine models and observations. This approach involved selecting a case-study from an observational dataset at an Antarctic field site. To make it more likely that the simulation of the case with LES and SCM was reasonably successful, we followed the methodology as in Figure 1 to determine the exact case (discussed in sections 2.5 and 2.6). The selection criteria dictated that the case study could be relatively simply initialised and forced (including the geostrophic wind and surface cooling rates). Ideally these forcings should vary little over the period of the case-study. Periods when such criteria were met were identified using European Centre for Medium-Range Weather Forecasts (ECMWF) analyses (to assess the wider synoptic situation), sodar profiles (to check the evolution of the boundary-layer structure), and the mast observations. Figure 1 describes the general choice between prescribing surfaces fluxes or temperatures. In the remainder of the study, we will prescribe surface temperatures.

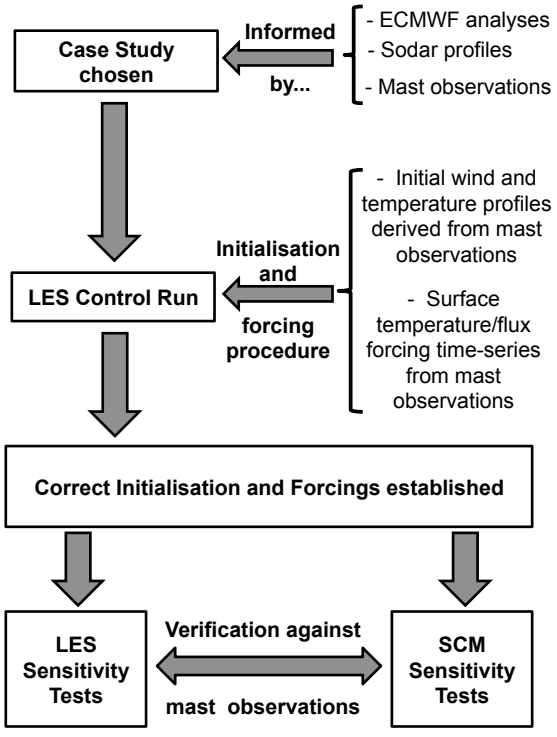

Figure 1. A flow diagram of the methods by which SCM, LES, and the field observations were coherently employed within the same project.

Having identified potential case-study periods, a control run to establish the correct initialization and forcings was performed using the LES. The LES was used in preference to the SCM for this purpose since the former have been shown to produce better simulations of moderately-stable boundary layers (Cuxart et al. 2006). The LES explicitly resolves the 3D turbulence, so is thus a better choice than the SCM where no turbulence is resolved. The LES was initialised using the mast observations. Once a case-study was modelled reasonably successfully, with a known initialisation and forcings, it was possible to use these to conduct sensitivity tests with both the LES and SCM. These sensitivity tests were mostly focused on the boundary-layer parameterization schemes. The model output from these tests was verified against the mast observations from the field site.

It is believed that the above procedure represents a powerful framework as to how to verify model results against a range of *in-situ* observations. Whilst the observations permit verification of the model output, the models allow the sensitivity of the SBL to various parameters to be explored and understood.

2.2. Site description and observational dataset

Over the past several decades, the British Antarctic Survey have made boundary-layer observations from Halley Research Station, Antarctica (75^o 35'S, 26^o 50'W). Halley is situated in Coats Land, on the eastern side of the Weddell Sea. Coats Land is comprised of the Brunt Ice Shelf and the adjacent continent. Halley is 10 km from the seaward edge of the Brunt Ice Shelf, and 30 m above sea-level.

Previous observation-based studies of stable boundary layers in the mid-latitudes have encountered significant complications arising from inhomogeneous terrain and diurnal variations. In contrast, the Brunt Ice Shelf provides an excellent site for making boundary layer measurements by minimising these effects.

Firstly, the high latitude of the site, combined with a high surface albedo, means that stable conditions predominate in the boundary layer for six months of the year, with only small diurnal variations. Surface-based temperature inversions occur during much of the year, and can reach strengths of 1 Km^{-1} under light wind conditions (King and Anderson 1988). Secondly, the prevailing surface wind at Halley is from the east, meaning that for most of the time there is a uniform fetch of about 40 km between the observing station and the closest irregular terrain. Thirdly, the surface of the ice shelf surrounding Halley is smooth and extremely flat (1:2000 slope, King et al. 1989). The consequence of this is that boundary layers formed here are among the closest to equilibrium found anywhere on Earth.

The Halley site is particularly configured to making high-quality observations of the SBL. These began in 1986, with the STable Antarctic Boundary Layer Experiment (STABLE, King and Anderson 1988). Further technical details are outlined in King and Anderson (1994). The observations presented in this study were all made during 2003, when several additions and improvements had been made to the STABLE instrument suite in the light of experience and technological advances.

A 32 m instrument mast was deployed at Halley, upon which instruments were mounted to measure both mean and turbulent profiles of meteorological variables. The mast was sited approximately 400 m south-east of the main base buildings. Such a position ensured that the base buildings did not obstruct surface winds blowing from north-east through south-west. Since the strong radiative cooling at high latitudes supports the formation of shallower, more stable boundary layers than are found at mid-latitude sites (Kottmeier 1986), observational arrangements are simplified. In particular, a relatively short instrument mast can be used to profile a larger proportion of the boundary layer. A summary of the mast instrumentation is provided in Table 1.

Parameter	Sensor heights [m]	Instrument
Wind speed	1, 2, 4, 8, 16, 32	Cup anemometer *(R.M. Young propeller)*
Wind direction	1, 2, 4, 8, 16, 32	Wind vane *(R.M. Young vane)*
Absolute temperature	1, 2, 4, 8, 16, 32	Platinum resistance thermometer *(Vaisala HMP45)*
Turbulent fluxes of heat	4, 16, 32	Sonic anemometer *(Metek GmbH USA 1)*
Turbulent fluxes of momentum	4, 16, 32	Sonic anemometer *(Metek GmbH USA 1)*

Table 1. Summary of observed variables and instruments used on the 32 m mast at Halley Station.

2.3. Description of the large-eddy model

This study uses Version 2.4 of the Met Office LES Model (Gray et al. 2004) to simulate the boundary layer at Halley. The general principles underpinning large-eddy models are described in Pope (2000). The Met Office LES Model has a strong record in successfully simulating moderately stable boundary layers, and guiding parameterization schemes (see Beare and Macvean 2004; Beare et al. 2006b). Full details on this model are outlined in Mason (1989) and Brown et al. (1994). The Met Office LES Model solves the filtered Navier-Stokes Boussinesq equation, set for use in dry boundary-layer simulations. The sub-grid model parameterizes the effects of turbulence occuring on scales smaller than those which are explicitly resolvable. The form this takes in the Met Office LES Model is described in Gray et al. (2004).

2.4. Description of the single-column model

The single-column model employed in this study used a first-order turbulence closure and was run at high vertical resolution. It incorporates turbulent parameterizations which are very similar to those used in numerical weather prediction and climate models. We model an area-averaged zone of the atmosphere which is represented by a one-dimensional set of equations. The atmosphere is assumed to be dry and divergence of radiative fluxes is neglected in the energy equation in the boundary layer. Both assumptions are confirmed as reasonable simplifications for the Antarctic atmosphere as a consequence of the low temperature and high long-wave emissivity of ice and snow surfaces (Handorf et al. 1999), although radiation remains important for the surface energy balance. In a dry, horizontally-homogeneous boundary layer, and in the absence of radiative flux divergence, the Reynolds averaged equations describing the dynamics of the atmospheric boundary layer can be written as

$$\frac{\partial \overline{u}}{\partial t} = f(\overline{v} - v_g) - \frac{\partial \overline{u'w'}}{\partial z}, \tag{1}$$

$$\frac{\partial \overline{v}}{\partial t} = f(u_g - \overline{u}) - \frac{\partial \overline{v'w'}}{\partial z}, \tag{2}$$

$$\frac{\partial \overline{\theta}}{\partial t} = -\frac{\partial \overline{w'\theta'}}{\partial z}, \tag{3}$$

where the variables in Equations (1) - (3) are defined in Table 2. Overbars indicate an ensemble mean. The subscript g refers to the geostrophic component of the flow. (1) - (3) contain more unknowns than equations: this is known as the turbulence closure problem. To complete this system of equations, a model for turbulent fluxes is thus required. The simplest method to model turbulence in the Reynolds-averaged equations is known as first-order closure, and represents the flux term in each mean-field equation through an eddy-diffusivity in the following way:

$$\overline{u'w'} = -K_m \frac{\partial \overline{u}}{\partial z}, \tag{4}$$

$$\overline{v'w'} = -K_m \frac{\partial \overline{v}}{\partial z}, \tag{5}$$

$$\overline{w'\theta'} = -K_h \frac{\partial \overline{\theta}}{\partial z}, \tag{6}$$

where K_m and K_h are the eddy diffusivities for momentum and heat respectively. All the complexities of turbulence are encapsulated by these diffusivities and are specified by making use of the following mixing-length model for stable conditions (Louis 1979).

$$K_m = \lambda_m^2 S f_m(Ri), \tag{7}$$

$$K_h = \lambda_h^2 S f_h(Ri), \tag{8}$$

where λ_m and λ_h are the mixing lengths for momentum and heat respectively, S is the vertical wind-shear, and f_m and f_h are stability functions dependent on Richardson number (Ri) (Beare and Macvean 2004). The mixing length formulation is described in Section 5.1. The formulation of stability function is a crucial choice in parameterizing the stable boundary layer. Four well-established stability functions are defined mathematically in Appendix 5.2, and are referred to in the text as the "cut-off" , "sharp tails" , "Louis tails" , and "long tails" schemes. Their stability-dependence is displayed graphically in Figure 2. For small, positive Richardson numbers, these stability functions can be determined from Monin-Obukhov theory. However, classical Monin-Obukhov theory predicts that a laminar flow will become turbulent when the Richardson number falls below a certain critical value, Ri_{cr} (Miles 1961). A value of 0.25 is normally assumed (Stull 1988). (17) and (18) both broadly follow this condition.

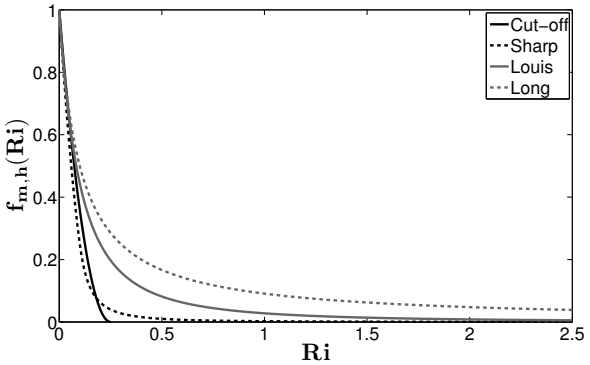

Figure 2. Graphical representation of the Ri-dependence of stability functions tested in this study.

Two issues exist with this view. Firstly, laboratory experiments have demonstrated that turbulence can exist in the SBL for Richardson numbers in excess of this critical value (Kondo et al. 1978). Secondly, the use of stability functions in operational NWP models which adhere to the concept of a critical Richardson number are associated with poor model performance. These problems include unrealistic, "runaway" surface cooling (Derbyshire 1999), and insufficient Ekman pumping (Beljaars and Viterbo 1998). Operational NWP models work around this problem by utilising stability functions with so-called "enhanced mixing", which artificially support turbulent mixing at higher stabilities (Beljaars and Holtslag 1991). (19) and (20) are two such examples. This solution is, however, rather unsatisfactory since it is inspired by model performance rather than laboratory and observational data. Furthermore, for very stable boundary layers the use of such enhanced mixing functions can degrade model performance by, for example, leading to an overestimate in the 2 m temperature.

Variables are stored on a staggered, Lorenz grid (the same as the Met Office LES model), with mean and turbulent variables on alternate levels. This is beneficial, since turbulent fluxes are parameterized in the SCM in terms of gradients of mean variables (see (4)-(6)). Thus, the use of a staggered grid effectively doubles the vertical resolution. Our vertical grid uses a logarithmic spacing of levels (Weng and Taylor 2003), resulting in very fine resolution close to the surface. The grid spacing enabled a wind profile that was close to logarithmic in the surface layer. This also enables the sharp surface-layer temperature gradients to be captured, and the surface fluxes to be accurately represented.

The surface boundary conditions are no-slip (u = v = 0 at the surface), with a specified time-dependent surface temperature. Ideally, a land-surface scheme should be used at the bottom boundary. However, the Antarctic boundary layer is sufficiently complex that we decided to focus on the interior mixing, and prescribe the surface temperature. Once the above-surface mixing is understood, the land surface can be included in future studies. In this study, this surface temperature timeseries was based on observations from the Halley site. The numerical scheme employed here for time integration is Crank-Nicolson. This method is implicit with second-order accuracy.

t	time
u_g, v_g	horizontal geostrophic wind speed components
u, v	horizontal wind speed components
u', v', w'	horizontal and vertical components of wind velocity perturbation
θ	potential temperature
θ'	potential temperature perturbation

Table 2. Definition of the variables used in the SCM equation set (1), (2), and (3).

2.5. *LES and SCM setup*

Following the methodology outlined in Section 2.1, a case-study was selected from the dataset of observations from Halley and used to initialise, force and validate the LES and SCM. The case study focused on the evening of 29 October, 2003, during the austral spring. At this time of year, some solar forcing was present, producing a diurnal cycle in the Halley boundary layer.

Section 2.1 has outlined the strategy developed by, and employed in, this study for using observations to validate numerical model results. To summarise this strategy, the observations were first used to initialise an LES control run. The aim of this control run was to establish the correct initialisation and forcings prior to conducting sensitivity tests using the single-column model. It also provided a robust method of obtaining initial profiles above the height of the instrumented mast. The details of this model run are summarised in Table 3, and the choices explained further below.

SBL simulations are very sensitive to the choice of initial conditions, and appropriate attention must consequently be given to any initialisation procedure. The model's initial potential temperature profile is displayed in Figure 3. To stimulate turbulence, this profile was subjected to random perturbations up to a height of 50 m (see Mason and Derbyshire 1990). The initial perturbations are confined to just this shallow layer in order that the LES can establish its own boundary layer with time.

This initial temperature profile was established in the following way. By 18 UTC, a well-defined, linear surface-inversion was evident in the profile mast observations. These observations were used to calculate the surface lapse-rate, and this lapse-rate was used to extend the inversion up to the top of the boundary layer. The boundary-layer depth was established using sodar observations (see section 2.6). In the absence of any temperature observations above the boundary-layer top, a climatological isothermal lapse-rate was used thereafter. This approach had some similarities to that used by Kosovic and Curry (2000), who used an idealised initial temperature profile which evolved into the observed profile. The case presented in this manuscript was, however, much more strongly linked to observational data. The LES was forced using a prescribed surface temperature time-series. This time-series was established by linearly extrapolating the temperature profile from the instrumented mast down to the surface. We performed sensitivity tests to the initial boundary layer depth, and found that the one prescribed was optimal.

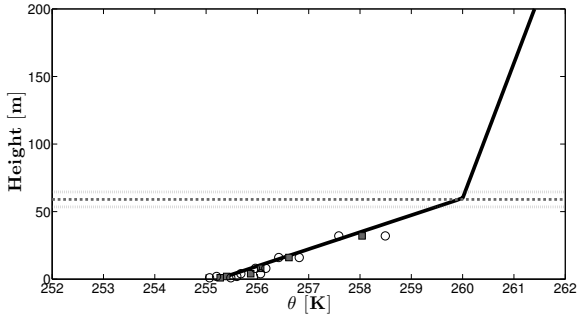

Figure 3. Initial potential temperature profile for case study. The model profile is indicated by the solid, black line. The grey square markers show the observed, one-hour averaged, potential temperature. Circular markers indicate one standard deviation either side of this mean for the observations. The boundary-layer depth (derived using the sodar data) is overplotted with the grey dashed line; one standard-deviation either side of this mean is indicated by two dotted grey lines.

Model domain: (horizontal x horizontal x vertical) [m x m x m]	(208 x 208 x 200)
Vertical grid length [m]	1.75
Horizontal grid length [m]	3.25
Surface forcing	Prescribed surface temperature time-series
θ_{ref} [K]	255.3
Wind speed initialisation	Constant geostrophic wind with height (zero at the surface)
Geostrophic wind: u_g, v_g [ms^{-1}]	-7.5, -1.5
Roughness length [m]	1.1×10^{-4}
von Karman constant	0.4
Gravitational acceleration [ms^{-1}]	9.81
Coriolis parameter [s^{-1}]	-1.408×10^{-4}

Table 3. Details of LES control run for the case study.

The mast observations were also used to determine the wind forcings applied in the model. This data led to a value for u_g of -7.5 ms^{-1} being selected. The choice of v_g was a more difficult decision, given the variability present in the observations at even the 32 m level. After consulting the radiosonde profiles, a value of -1.5 ms^{-1} was chosen. These initial wind profiles were constant at all model levels. These values for the geostrophic wind speed were held constant for the duration of the case study.

Applying the correct roughness length in a numerical model is also an important consideration. Careful prescription of roughness length allows turbulence to be accurately generated by shear, and, in turn, realistic boundary-layer profiles produced. In the experiments in this study, the well-established value for Halley (1.1×10^{-4} m, King 1990) was used.

For the stability function sensitivity tests, presented in Section 3.2, the SCM was initialised and forced as the LES control run (Table 3). The only difference between the SCM and LES was the vertical grid; the SCM has a grid length of 1 m in the surface layer which increased logarithmically above.

2.6. *Rationale for case selection*

This particular day was selected for use as a case-study for a number of reasons, detailed here. Firstly, the presence of a diurnal cycle meant that the numerical models could be initialised just

after the evening transition. This made for a simpler initialisation of the temperature profile, since the surface inversion was well-defined at this time (the boundary layer being well-mixed, prior to the onset of the evening transition). The instrumented mast observations showed that the strength of the surface inversion increased markedly over the period of the case study (18-24 UTC), with the difference between the 1 m and 32 m measurements being 2.5 K at 18 UTC, but approaching 9 K six hours later. The average temperature difference between these levels for October 2003 was at the lower end of this range (2.6 K), with the annual average for 2003 being slightly more strongly stratified (3.6 K).

This case study considers stratifications which, although above average, are commonly observed at Halley. Indeed, the more strongly-stratified boundary layers are arguably more interesting from a parameterization viewpoint; the high-stability limit is typically the most challenging for parameterization schemes (Mahrt 1998). Thus, although the stratifications considered in this case study may be above average in strength, improvements to parameterizations in this regime may be expected to yield a greater impact than those developed for the neutral regime. Also, the clear trend in surface temperature over the nocturnal period also simplified the surface forcings. The observations show that the surface temperature (approximately indicated by the 1 m observations) cooled monotonically over this same period.

The second reason for selecting this case study was that the profile mast observations and mean sea level pressure (MSLP) charts both indicated that the geostrophic winds were relatively constant for the duration of the case study. This simplified the wind forcing of the models. The mast observations showed that the u-component of wind speed was moderate in strength (-7.5 ms^{-1} at 32 m), and reasonably constant in magnitude over the period of the case-study. The v-component of wind speed fluctuated between -1 and +2 ms^{-1}. The observed wind magnitude for this case study was 7.6 ms^{-1}. This was slightly weaker than both the October 2003 average (8.1 ms^{-1}) and 2003 annual average (7.7 ms^{-1}). The combination of wind-speed components which prevailed during this case study produced an easterly airflow over Halley. The time series of wind observations display various small oscillations which provide further challenges when attempting to model this boundary layer.

These wind direction observations were confirmed by mean sea level pressure charts for 18 UTC, 29 October and 00 UTC, 30 October. Figure 4 displays these MSLP charts, based upon ECMWF re-analyses data (British Atmospheric Data Centre 2012). The approximate location of Halley Station on these charts is indicated by a cross symbol on each. Low pressure systems are situated to the north-west and north-east of Halley, with higher pressure lying to the south. These charts show that the synoptic situation remained relatively unchanged over the period of this case-study.

In addition to these practical reasons for selecting this case-study, evening transitions are important phenomena whose dynamics remain incompletely understood (Beare et al. 2006a). Since transitions feature a range of shears and stratifications, they offer a good opportunity to assess the performance of stability functions. The study of such a boundary-layer at Halley is thus an interesting challenge in itself.

The sodar profiles during the case study were analysed to gain an insight into the evolution of the boundary layer. Although an uncalibrated instrument, this data was useful for confirming the relatively constant turbulent profiles over the period of this case study. These data indicated that the boundary layer remained approximately 60 m deep throughout the period of the case study.

To summarise, in this investigation a case study was considered from the Halley dataset. This case study occured during the austral spring of 2003. At this time of year, there was some diurnal

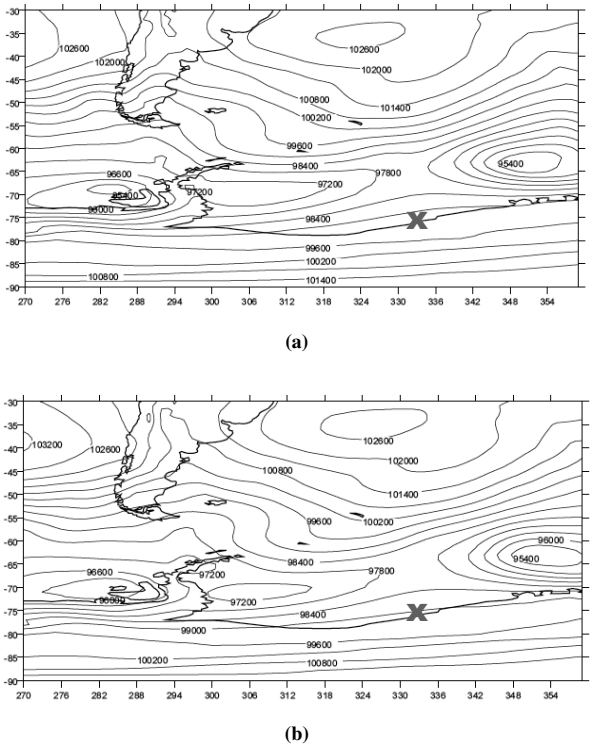

Figure 4. Charts of mean sea level pressure for (a) 18 UTC, 29 October 2003, and (b) 00 UTC, 30 October 2003. Pressure is plotted in Pa. The approximate location of Halley Station is indicated by a grey cross on each chart, and experiences only weak synoptic forcing over the period of this case-study. British Atmospheric Data Centre (2012)

cycle in insolation. The model was initialised just after onset of the evening transition, since this simplified the initialisation procedure. The diurnal cycle produced a clear variation in surface temperature, which resulted in an increase in the degree of stratification over time. There was little synoptic forcing during this case study, reducing the likelihood of a rapid change in air mass and making the wind forcings relatively constant during the period of interest. This case thus presented the opportunity to model a stable boundary layer with reasonably constant wind forcings, but with variable stratification.

3. Results

The large-eddy model results are presented in Section 3.1. The sensitivity of the SCM results to the formulation of stability function is investigated in Section 3.2. Stability functions, as implied by the LES, are described in Section 3.3. Throughout the paper, we will compare hour-averaged vertical profiles for the LES and observations.

3.1. LES control simulations

Figure 5 shows the wind profiles produced by the LES at 22 UTC, four hours after initialisation. Since there was a weak diurnal cycle, four hours of simulation represented a reasonable middle of the night time for verification, and sufficient time for the LES to establish a boundary layer. The sodar-derived boundary-layer depth is also over-plotted. It is apparent from Figure 5 that good agreement between the LES control run and observations has been achieved. The profile for the v-component very closely matches the observed profile. In Table 4 we quantify the root mean squared error of the LES using

$$\sqrt{\frac{\Sigma_{\mathrm{o}}(\theta_m - \theta_{\mathrm{o}})^2}{N_{\mathrm{o}}}}, \tag{9}$$

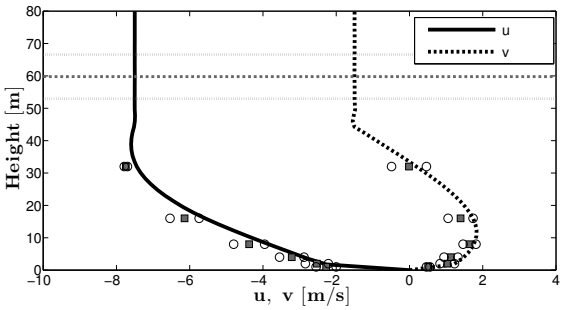

Figure 5. Profiles of horizontal wind speed components from the LES control run and observations four hours after initialisation. u/v wind components from the LES are displayed by the solid/dashed lines respectively. All markers/lines as for Figure 3. Both LES and observed profiles are one-hour averages.

Potential temperature	u wind	v wind
1.15 K	0.41 ms^{-1}	0.26 ms^{-1}

Table 4. Root-mean squared errors of LES variables when compared with the mast observations.

where Σ_{o} indicates a summation over observed points, subscript m indicates LES values interpolated onto observed points, and subscript o is for observed points, where N_{o} is the number of observed points. The same calculation is applied to the horizontal wind components. The LES may, however, be slightly underestimating the strength of the maximum in the u-component of wind speed. This problem may be attributed to small errors in the wind forcing and the possible impact of phenomena such as gravity waves, as well as limitations in the model. Disentangling these possibilities is difficult to achieve, however. It is also unclear from the observed profile whether the model has placed this jet at precisely the correct height. The observations are unable to definitively confirm the jet height, since they only extend to 32 m. Overall, however, there is good agreement between the model and observations for wind speed. We note that this doesn't necessarily imply a close agreement in other diagnostics (see later). It should also be remembered that the relative shallowness of high-latitude boundary layers has allowed a greater proportion of the boundary layer to be profiled here than would be possible at a mid-latitude location with a mast of such size.

When the model results and sodar observations are compared, the LES also appears to predict a slightly shallower boundary-layer depth. This may, however, be partly attributed to the method by which the sodar calculates this boundary-layer depth. This is defined as the height at which the backscattered sodar signal drops to 30% of its near-surface value, divided by 0.7. This calculation assumes a linear variation with height; so, in shallow boundary layers, such a threshold may lead to a systematic over-estimate of boundary-layer depth as the variation can be curved. Also, since sodar primarily detects small-scale temperature variations, the sodar normally identifies the top of the inversion layer. Generally, this height is different to the height of a boundary-layer depth defined in terms of turbulent profiles.

The potential temperature profiles for this model run are shown in Figure 6. The form of the surface inversion at Halley was frequently non-linear. Figure 7 graphically illustrates the definitions used in this study when discussing the phenomenon of potential temperature curvature. Given these definitions, the observed profile in Figure 6 displays a marked positive curvature between 5 and 40 m above the surface. In contrast, the LES profile is both too linear and shows a surface inversion which is weaker than that which was observed. The larger potential temperature gradient in the lowest 5 m of the LES is consistent with the surface sensible heat flux and surface similarity. The differences for the potential temperature are larger than for the winds. Whilst the potential temperature and wind speed are intrinsically coupled in the SBL, their initialisation and surface boundary conditions are known with different levels of certainty. This is the likely reason for the better agreement with observations for LES winds than the potential temperature.

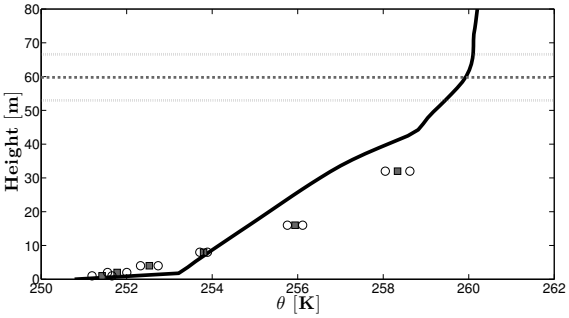

Figure 6. Profile of potential temperature from the LES control run and observations four hours after initialisation. All markers/lines as for Figure 3. Both LES and observed profiles are one-hour averages.

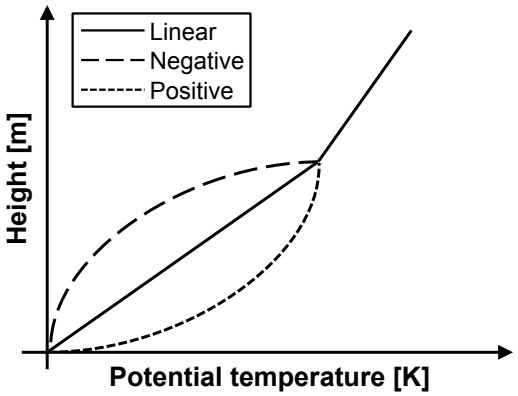

Figure 7. Illustration of definitions for potential temperature profile curvature used in this study. Three profiles are plotted: a linear profile; a profile with negative curvature; and a profile with positive curvature.

Figure 8 displays the corresponding momentum flux (square-rooted) profiles for this case. It should be noted that, even after averaging, flux observations do tend to be more time-variable than mean observations (such as wind speed). Despite this variability, reasonable agreement has still been achieved between the LES and observed profiles. Howevever, the LES has slightly over estimated the surface friction velocity (0.11 ms^{-1}) compared to the observed value (0.08 ms^{-1}).

Finally, the heat flux profiles are shown in Figure 9. Heat flux profiles are the most time-variable measurement considered in this study. Both the observed and modelled data show typical profiles for heat flux in the stable boundary layer: a negative value at the surface, declining approximately linearly to zero at the top of the boundary layer. However, the magnitude of the surface heat flux seems to be underestimated by the LES compared to the observations (-5.5x10^{-3} K.ms^{-1}, as compared to -8.2x10^{-3} K.ms^{-1}). In addition, the vertical gradient of heat flux from the LES is noticeably smaller than that in the observations. This is associated with the differences in the lapse-rate in potential temperature noted in Figure 6.

There is also some evidence from Figure 9 that the LES is over-estimating the boundary-layer depth, if the boundary layer

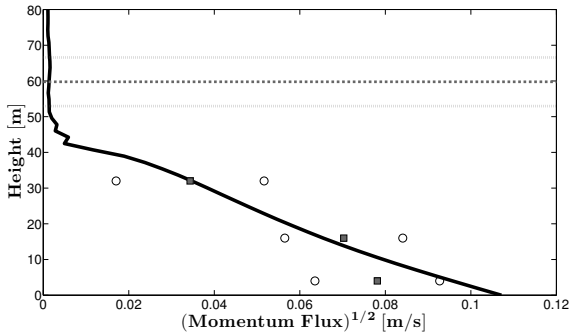

Figure 8. Profile of momentum flux (square-rooted) from the LES control run and observations four hours after initialisation. All markers/lines as for Figure 3. Both LES and observed profiles are one-hour averages.

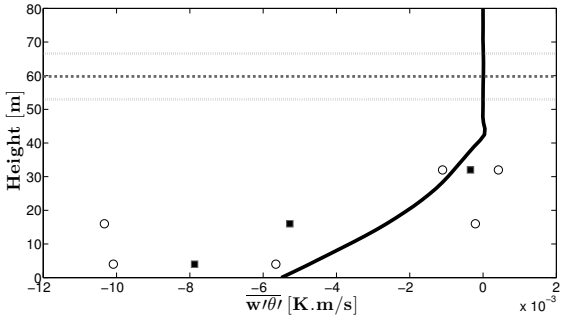

Figure 9. Heat flux profiles from LES control run for case study, four hours after initialisation. All markers/lines as for Figure 3. Both LES and observed profiles are one-hour averages.

depth deduced from the heat flux observations is considered more reliable than the sodar. As previously commented, in the classical stable boundary layer the heat flux declines to zero at the boundary layer top (Stull 1988). The observed heat flux profile indicates that the heat flux is approximately zero at 32 m. In contrast, the LES only approaches this point at 45 m.

For this model run, more than 70% of the heat flux in the interior of the flow was explicitly resolved. Naturally, this proportion is resolution-dependent, with the results becoming more reliant on the sub-grid model at coarser resolutions. Initial investigations whilst setting up this model run indicated that the grid-lengths used here were a satisfactory balance between resolution and computational speed.

Overall, this LES control run was reasonable at modelling mean and turbulent profiles compared to observations. The degree of agreement between model results and observations both gives us confidence in using these initialisations and forcings in future model runs, and provides a solid control run which can be used as a reference when discussing the results from sensitivity tests in the next section.

3.2. Stability function sensitivity tests

Section 2.4 described the difficulties involved in parameterizing turbulence in weather and climate models. In these models, this issue largely hinges upon the formulation of the stability functions used. This choice of stability function is far from straightforward, with a large number of competing variants having been proposed. In Section 3.1 the LES and observations were used to establish and test the initial profiles and model forcings for the case study. In the following section, four stability function formulations (Figure 2) were tested in the SCM against the observations. These stability functions are defined by (17) - (20), respectively.

The wind profile results from four hours after the initialisation are presented in Figure 10. Compared to the LES, all configurations of the SCM performed worse when compared to the observed wind profiles. The longer-tailed functions are designed to produce enhanced turbulent mixing at higher stabilities, thereby yielding deeper boundary layers. The sharp and cut-off stability functions performed best against the observed profiles. Against the u-component observations, neither the cut-off nor the sharp tails produced strong enough near-surface wind shear, and the wind speed maximum in each occured at a greater height than where the observations indicated it was likely located. In the v-component, the sharp tails produce the profile which is closest to the maximum observed wind speed. However, both the sharp and cut-off tails spread this jet over an excessively deep layer.

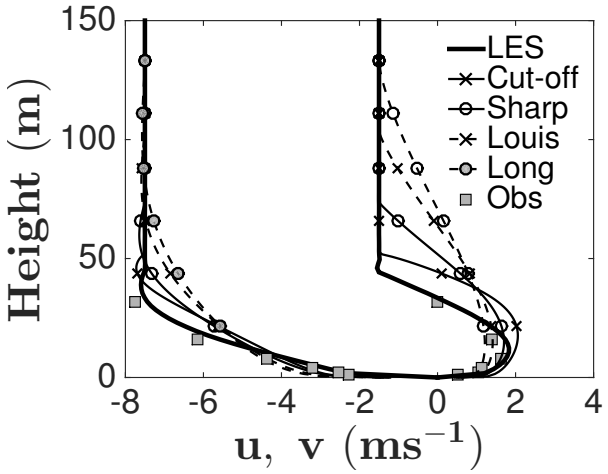

Figure 10. Horizontal wind speed component profiles for the SCM stability function sensitivity tests (u components on the left and v components on right), four hours after initialisation. Results are plotted from the SCM using cut-off, sharp, Louis and long-tailed schemes. Profiles from the LES control run are also plotted for reference, along with the mean observed profiles. Both LES and observed profiles are one-hour averages.

Figure 11 displays the sensitivity of the potential temperature profile to stability function, which has an impact on turbulent mixing within the SBL. The range of curvatures present in the temperature profiles is also noteworthy. Although the cut-off and sharp tailed functions both simulated shallower boundary layers than the longer-tailed schemes, their temperature profiles above the surface layer exhibited negative curvature. This was in the opposite sense to the observations. In contrast, the long and Louis schemes produced curvature in the same sense as the observations, although the greater degree of mixing that these schemes stimulated also resulted in an overly-deep boundary layer. The consequence of this is that the overall agreement with the potential temperature observations was poorer for the long/Louis-tailed results than the cut-off/sharp schemes. None of the four functions trialled here succeeded in producing a surface inversion which was as strong as was observed.

The momentum flux (square-rooted) profiles for this sensitivity test are plotted in Figure 12. All four stability function schemes make a large over estimate of the surface value of momentum flux (square-rooted). The cut-off tails produce a surface momentum flux (square-rooted) of 0.13 ms^{-1}, whilst the long tails predicted a value of 0.14 ms^{-1}. The observed value was only 0.08 ms^{-1}. In general, the trend was for the longer-tailed schemes to predict a larger surface momentum flux (square-rooted) and a smaller vertical gradient in momentum flux (square-rooted). Both of these can be attributed to the enhanced mixing inherent with longer-tailed schemes. Although the difference in surface values between the cut-off model results and observations was quite large, this

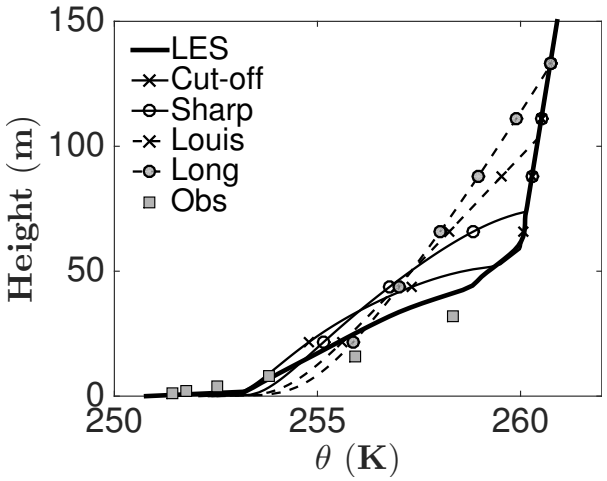

Figure 11. Potential temperature profiles for the SCM stability function sensitivity tests and LES control run, four hours after initialisation. All markers/lines as for Figure 10. Both LES and observed profiles are one-hour averages.

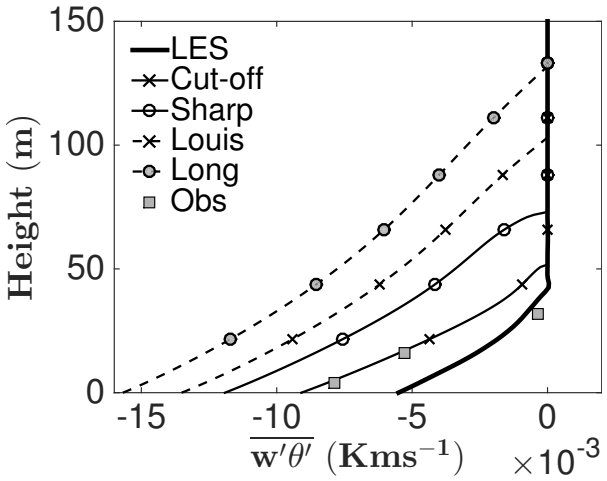

Figure 13. Heat flux profiles for the SCM stability function sensitivity tests and LES control run, four hours after initialisation. All markers/lines as for Figure 10. Both LES and observed profiles are one-hour averages.

discrepancy was much smaller above the surface. For example, the difference at 32 m between the cut-off tail results and observations was only 0.02 ms^{-1}. In contrast, the discrepancy between the long tails results and observations at the same height was 0.06 ms^{-1}.

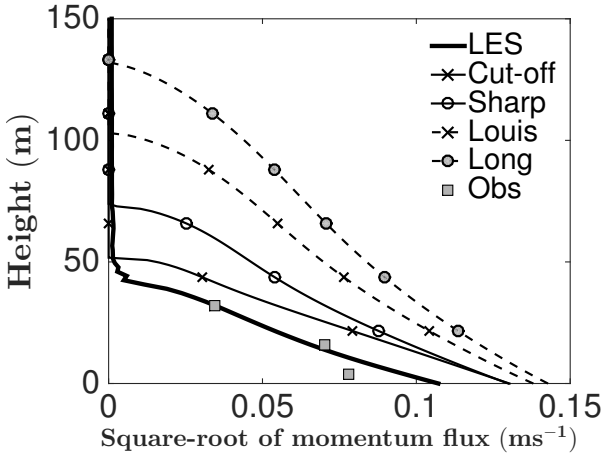

Figure 12. Momentum flux (square-rooted) profiles for the SCM stability function sensitivity tests and LES control run, four hours after initialisation. All markers/lines as for Figure 10. Both LES and observed profiles are one-hour averages.

x

Figure 13 shows the heat flux profiles for the same time. Figure 13 indicates a similar picture to Figure 12: namely that longer tails result in larger surface flux values and deeper boundary layers. In the case of heat flux profiles, the cut-off tails produced a surface value which was very close to the observed value (-9x10^{-3} K.ms^{-1}). In contrast the long tails version of the model predicted a surface value of -1.6x10^{-2} K.ms^{-1}. However, even the cut-off tails scheme struggled to generate a sufficiently strong heat flux gradient with height.

Figure 14 shows a time-series of boundary-layer depths from the four configurations of the SCM. The sodar observations of boundary-layer depth are also plotted for reference, as are the results from the LES control. Note that the first hour of results have been omitted to remove the post-initialisation adjustment phase. The definition of boundary-layer depth used with the model results was the height at which the momentum flux (square-rooted) dropped to 5% of its surface value, divided by a scaling-factor of 0.95. This is the same method used by Kosovic and Curry (2000). As has been previously described, the sodar defined the top of the boundary layer as the point at which the backscattered sodar signal dropped to 70% of its surface value. This height was strongly dependent on temperature structure, and this difference in definitions of boundary-layer depth means that the two datasets are not directly comparable. It is still included, however, as a useful reference in the absence of any direct observations from above 32 m (the top level of the instrumented mast).

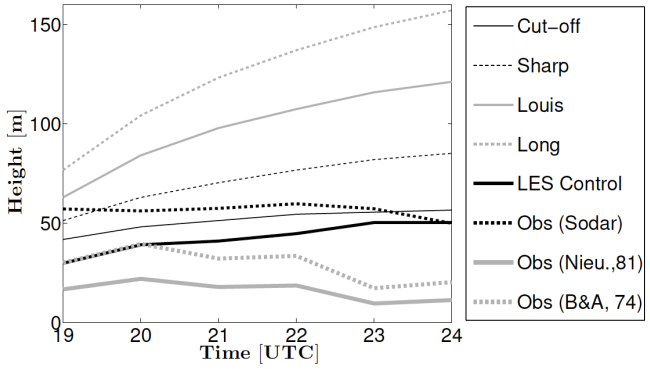

Figure 14. Boundary-layer depth time-series from the stability function sensitivity tests. Boundary-layer depths were diagnosed from the model results by the height at which the momentum flux drops to 5% of its surface value, divided by 0.95. Results from the cut-off, sharp, Louis and long-tailed configurations of the SCM are plotted, along with the LES control results. Boundary-layer depth observations from the sodar, and the predictions of Nieuwstadt 1981 and Businger and Arya 1975 are also plotted for comparison.

Also plotted on Figure 14 is a definition for boundary-layer depth first derived by Zilitinkevich (1972):

$$h = \gamma \sqrt{\frac{u_* L}{f_0}}. \tag{10}$$

where L is the Obukhov length, defined thus:

$$L = \frac{-\bar{\theta} u_*^3}{kg\left(\overline{w'\theta'_0}\right)}. \tag{11}$$

and u_* is the friction velocity:

$$u_*^2 = \left(\overline{u'w'_0}^2 + \overline{v'w'_0}^2\right)^{0.5}. \tag{12}$$

In (10), γ is a constant of proportionality. There is some discussion regarding the value γ should assume. Businger and Arya (1975) suggested a value of 0.72, whilst Nieuwstadt (1981)

favoured 0.4. This range of values is indicative of the difficulty in diagnosing the depth of the SBL. Accordingly, results using both of these values are displayed in Figure 14. (10) is defined in terms of quantities measured by the instrumented mast, and provides a second measure of boundary-layer depth based on observations. These definitions yield boundary-layer depths of 10-20 m (Nieuwstadt 1981) and 20-40 m (Businger and Arya 1975) for the case study. When the observed mean and turbulent profiles are considered, both values of γ appear systematic underestimates.

The reason for this under estimate is probably linked to the size of u_*. The value used in (10) was based on the measurement from the lowest level of the instrumented mast (4 m). For the case study this was 0.07 ms^{-1}. This value is rather smaller than that seen in other case studies using the Halley observations (not shown here), whilst the magnitude of the surface heat flux was similar to that found in this case.

The sodar time-series indicates that the boundary-layer depth remained remarkably constant over the period of the case-study (60 m). Figure 14 shows the sodar's boundary-layer depth lay close to that simulated by the sharp and cut-off tails configurations of the SCM. Both the Louis and long tails produced a significant over estimate in the height of the boundary layer. All four tails configurations produced a deeper boundary layer than the LES control run.

The data contained in Figure 14 serves to strengthen the conclusions which the profile results (Figures 10 - 13) indicated - namely that the longer tails produce excessive mixing, exerting a detrimental impact on profile structure and resulting in the development of an overly-deep boundary layer.

3.3. *Implied stability functions from LES*

Beare et al. (2006b) used LES to guide the choice of stability functions for SBL parameterizations. In the following section, the approach of Beare et al. 2006b was used to analyse the results from the Halley case study. As was introduced in Section 2.4, weather and climate models commonly employ eddy-diffusivities for momentum and heat to parameterize turbulence (Equations 7 - 8). Although LES explicitly resolve the larger turbulent eddies, the LES data can be used to extract an effective momentum eddy diffusivity (K_m^{eff}), using the total momentum flux and mean wind profile. This approach yields the following expression:

$$K_m^{eff} = \frac{\left(\overline{u'w'}^2 + \overline{v'w'}^2\right)^{\frac{1}{2}}}{\left(\frac{\partial u}{\partial z}^2 + \frac{\partial v}{\partial z}^2\right)^{\frac{1}{2}}}. \tag{13}$$

(7) can be rearranged, and adapted to the parameters extracted from the LES to give

$$f_m^{LES} = \frac{K_m^{eff}}{\lambda_l^2 S}. \tag{14}$$

where λ_l is the mixing length for the LES, defined by

$$\frac{1}{\lambda_l} = \frac{1}{k\,(z + z_0)} + \frac{1}{\lambda_0}. \tag{15}$$

λ_0 is the asymptotic length scale of turbulence in the interior of the boundary layer. Beare et al. (2006b) investigated the sensitivity of results to the choice of this parameter and found considerable dependence. Beare et al. (2006b) used 40 m for their control. A smaller value is appropriate here because of the shallower, less-diffusive boundary layer which were considered. Scaling λ_0 with K_m^{eff} yielded λ_0 = 1 m.

Figure 15 displays the results for f_m^{LES} extracted from the LES control run. The data presented here provides further confirmation of the enhanced performance of the sharper-tailed stability functions. This conclusion concurs with that of Beare and his co-workers, although they only tested the sharp and long functions. The greater number of functions tested in this study permits a more robust comparison.

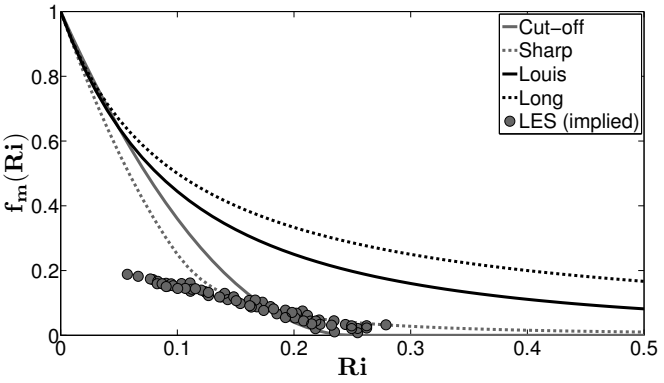

Figure 15. f_m extracted from the LES control run. Data from the LES case study are plotted with green square markers. For comparison purposes, the cut-off, sharp, Louis and long functions are plotted. The LES data strongly support the use of sharper-tailed functions.

3.3.1. *Comparison of results with GABLS-1*

Here, the Halley and GABLS-1 results are compared (Beare et al. 2006b). The GABLS-1 data were obtained using the Met Office Large-Eddy Model (2 m resolution), although these results were from 9 hours after initialisation. The set-up for GABLS-1 was loosely based on observations of an Arctic stable boundary layer, which was considerably deeper than those investigated in this study. The Halley profiles shown in this section are all from the LES control for the case study, four hours after initialisation.

In order to extract the implied stability functions, the LES-derived stress and shear profiles were combined using (13) to acquire an effective momentum eddy-diffusivity. Although the overall form of these profiles for Halley and GABLS was similar, the magnitude of K_m^{eff} was over an order of magnitude smaller in the Halley case (Figure 16). K_m^{peak} for the GABLS data agrees with that obtained by Shin and Hong (2011), who reported - under stable conditions - K_m^{peak} of 0.5-1.7 m^2s^{-1} for a range of boundary-layer schemes.

The significantly smaller values for K_m at Halley indicates that the SBL here is considerably more stable and shallower than the one considered in GABLS-1. When this value of K_m^{eff} is used in (14) it yields a much smaller value for f_m^{LES}. This explains the smaller values of f_m^{LES} with small Ri in Figure 15. The LES performs well for the Halley case despite this increased stability, possibly due to the continuous nature of the turbulence.

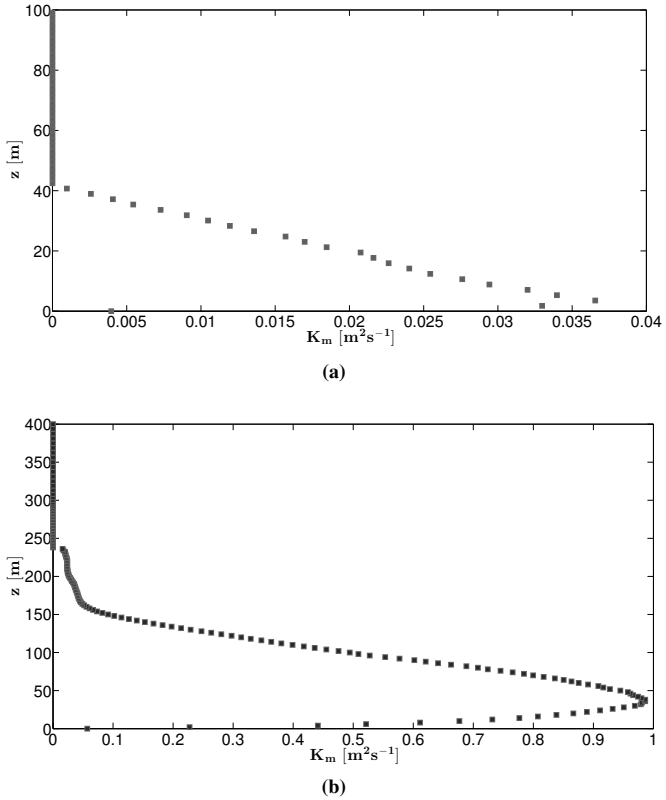

Figure 16. A comparison of LES-derived K_m^{eff} profiles from (a) Halley and (b) GABLS-1. This highlights the shallowness of the boundary layers found at Halley.

4. Discussion

In this paper, we presented modelling results from a case study based on observations from Halley, Antarctica. We used a framework that synthesised observations, a LES and a SCM. In this way we were able to understand more fully the mixing in stable boundary layers for the Antarctic region.

The LES was first used to model the case study. The purpose of this was to establish the correct initialisation and forcings, and to provide a reference for comparison purposes prior to conducting in further experiments. Good agreement between the LES and observations was achieved for up to four hours after initialisation. The wind profiles generally agreed well with the observations. Any slight differences were likely due to a combination of small errors in the wind forcings, the possible impact of advective effects and phenomena such as gravity waves, and limitations of the model. It is difficult to disentangle the relative impacts of these effects.

Reasonable agreement was also achieved between the modelled and observed potential temperature profiles. Small differences remained, however. Of particular note, the LES profile was rather too linear. This did not reflect the positive curvature of the observations. The surface inversion in the LES was also weaker above the surface layer than was observed.

Both the observed momentum and heat flux profiles were of the classical linear form. The momentum flux (square-rooted) was well-simulated by the LES, although the surface value of the heat flux was under estimated. These LES control runs generally achieved their twin aims. Firstly, they provided a means of establishing the correct initialisation and forcings, which were fully-justified by the observations. Secondly, they provided benchmark profile results for comparison purposes. We attribute these successes to the attention given to the initialisation and forcings used. Together with the high-quality, *in-situ* observations, the use of a high-resolution LES was invaluable in establishing these.

Using the initialisation and forcings established by the LES control runs, sensitivity tests were then conducted using the SCM to investigate the impact of stability function choice. As expected, it was found that longer-tailed schemes (which support more mixing at higher stabilities) resulted in the formation of deeper boundary layers. This yielded poorer agreement with the observed profiles. The sharp and cut-off schemes produced the best agreement with the observations.

The potential temperature results presented an interesting dilemma. Whilst longer tails produced positive curvature which mirrored that of the observed profile, they also resulted in a substantial over estimate in the boundary-layer depth. The cut-off and sharp schemes predicted negative curvature (the opposite of that which was observed) and shallower boundary layers. Overall, the consequence of this was that the cut-off and sharp schemes produced a closer match with the observations. However, none of the schemes tested simulated a strong enough surface inversion. The use of longer-tailed schemes resulted in the prediction of larger surface flux values and deeper boundary layers. The cut-off tail scheme performed strongest at simulating the flux profiles.

Stability functions were extracted from LES by Beare et al. (2006b). This approach was replicated in this manuscript. These results further reinforced the use of sharper-tailed stability functions. The results from Halley were then compared with those obtained by Beare and his colleagues as part of GABLS-1. These data showed that, in addition to the boundary layer being approximately three times as deep in GABLS-1, it was also substantially more diffusive than that considered in the Halley case study.

We attribute some of the improved performance of the LES to the treatment of turbulence within each of these models. Whereas the LES explicitly resolved the larger eddies, all the turbulent motions were parameterized in the SCM. This study has presented results which have highlighted issues surrounding the performance of these turbulence parameterizations schemes. In particular, sensitivity to stability function formulation has been investigated. Further sensitivites also exist to, for example, the choice of λ_0 (Beare et al. 2006b), Prandtl number (see Noh et al. (2003) for an example of a more robust treatment), and the order of turbulence closure model used (Mellor and Yamada 1982). Future research might fruitfully attempt to quantify these sensitivities.

We now compare the results presented in this study with those reported in previous studies and thereby set them in their wider context. Initially, the LES was used to obtain a control run for each case study. The predictions of these control runs were generally close to the observed profiles, and were successful in establishing the initial conditions and forcings. Basu et al. (2012) also used LES to study the stable boundary layer, as part of GABLS-3. In their case, they compared results from eleven LES against observations from a mid-latitude site. Their models were all remarkably successful in capturing the dynamical evolution of this boundary layer, with the diversity in the results from the ensemble being surprisingly low. This implies that the simulations were not very sensitive to the formulation of the subgrid model.

Basu et al. (2012) reported that their LES accurately captured the low-level jet, and the same could generally be said of the Halley results. Their LES experienced greater difficulty in simulating the low-level wind shear. Interestingly, however, this problem was not especially evident in the Halley results. Basu et al. (2012) also found that a relatively-coarse resolution (6.25 m) was adequate. A smaller grid length was used in both the vertical and horizontal for the simulations presented in this manuscript. The need for the higher resolution for the Halley case study can

be explained by a combination of the shallower boundary layers and stronger stratifications which develop in this high-latitude location.

Sensitivity to the formulation of stability function was extensively investigated in this manuscript, with implied stability functions being extracted from the LES control runs. As has already been mentioned, this technique was previously used by Beare et al. (2006b) for a deeper, Arctic boundary layer. The results in this paper are broadly consistent with the conclusions of Beare et al. (2006b), with sharper-tailed schemes offering improved performance. Beare et al. (2006b) did not test as many stability function formulations as were considered here. However, the decision to use a particular stability function operationally would need to be based on more case studies, covering a wider range of stabilities, than are presented in this study. Thus, the main conclusion is that these results, and those of Beare et al. (2006b), show that stability functions which employ enhanced mixing are unable to capture important aspects of near-surface wind and temperature profiles. The particular form that these sharper-tailed schemes should take will require further research.

King et al. (2001) also investigated the sensitivity to stability-function choice over Antarctica. In their case, however, they used a version of the Hadley Centre climate model, and focused on impacts on seasonal timescales. They found substantial sensitivities to the formulation of these functions, with corresponding impacts on momentum and heat fluxes, and the near-surface wind field. The authors highlight that this could have important implications for coastal sea-ice and deep-water formation processes. They suggest that the use of sharper-tailed schemes would lead to improved prediction of surface fluxes over the Antarctic continent, although they also admit that very few observations are available from this region to allow the development of appropriate stability functions. The need to increase the vertical resolution of climate models in order to capture shallow, high-latitude boundary layers is also identified as a priority.

Notable differences were seen between the modelled and observed profiles for the case study in this manuscript. Although the LES points towards some areas for development of the turbulence parameterizations used in the SCM, further convergence towards the observations might be achieved by including processes not considered by either model. Increasingly, the importance of radiation and land-surface interactions, alongside turbulent mixing, are being realised (Steeneveld et al. 2006a). A feel for the impact of such processes can be gained by looking at the results of previous work in this area.

Garratt and Brost (1981) investigated the impact of radiation on the evolution of the SBL. They found that the quasi-equilibrium SBL developed a three-layer structure. Radiative effects were found to dominate close to the surface, and near the top of the boundary layer. A key result was that radiative exchanges at the top of the SBL tended to weaken the inversion here and deepen the SBL by 20%. Steeneveld et al. (2006b) revisited the case used for GABLS-1, this time incorporating radiation and land-surface schemes in their model. Interestingly, they found for wind speeds similar to those of the Halley case study that the effect of radiation was minimal. At lower wind speeds (less than 3 ms^{-1}), however, the impact of radiation was far more significant.

Several studies have investigated the role of land-surface coupling in the SBL. Prescribing a surface temperature timeseries as the bottom boundary condition has limitations associated with it, and it does not fully reflect the complexities of the SBL dynamics (since the surface temperature, and surface energy balance are interdependent). That said, it is still a commonly-used approach and was used in the GABLS-2 intercomparison (Svensson et al. 2011).

Steeneveld et al. (2006b) trialled two land-surface schemes in their state-of-the-art SCM. The first solved the heat diffusion equation in the underlying ice. The second used a bulk conductance layer of stagnant air next to the surface. Both of these schemes produced shallower boundary layers than the reference case (which had no land-surface scheme).

Given that the SCM used in this study encountered particular difficulties capturing the shallowness of the SBL, the use of a fully-interactive land-surface scheme might be a fruitful path for future research. The case study considered in this manuscript was forced by a moderate geostrophic wind speed. However, the importance of both land-surface and radiative processes was recently reinforced by Sterk et al. (2013) for the low-wind speed regime. This implies that these processes should be borne in mind should future Halley case studies go on to consider such conditions.

5. Appendix

5.1. *Mixing length formulations*

The mixing lengths for momentum and heat, as employed in the SCM, are expressed in the following way:

$$\frac{1}{\lambda_m} = \frac{1}{\lambda_h} = \frac{1}{\kappa(z+z_o)} + \frac{1}{\lambda_o}. \tag{16}$$

where κ is the von Karman constant (0.4 is used in this study), z_0 is the roughness length and λ_0 is a constant neutral mixing length (a value of 15 m is adopted here). The form of Equation 16 ensures a smooth transition in λ between its expected near-surface value ($\approx \kappa(z+z_o)$), and the interior of the flow (where it asymptotes to λ_0).

5.2. *Stability functions formulations*

The four stability functions tested are defined mathematically below. These are referred to in the text as the "cut-off" , "sharp tails" , "Louis tails" , and "long tails" schemes respectively:

$$f_m = f_h = \begin{cases} \left(1 - \frac{Ri}{0.25}\right)^2 & 0 < Ri \leq 0.25 \\ 0 & Ri > 0.25, \end{cases} \tag{17}$$

$$f_m = f_h = \begin{cases} (1 - 5Ri)^2 & 0 \leq Ri \leq 0.1 \\ (\frac{1}{20Ri})^2 & Ri > 0.1, \end{cases} \tag{18}$$

$$f_m = f_h = \frac{1}{(1+5Ri)^2} \quad Ri \geq 0, \tag{19}$$

$$f_m = f_h = \frac{1}{1+10Ri} \quad Ri \geq 0. \tag{20}$$

Acknowledgement

The authors would like to thank Dr Philip Anderson (formerly British Antarctic Survey, currently at the Scottish Association for Marine Science) for his provision of the observations used in this study. KTW also acknowledges a University of Exeter studentship.

References

S. Basu, A. A. M. Holtslag, and F. C. Bosveld. GABLS3-LES Intercomparison Study. In *ECMWF Workshop on Diurnal cycles and the stable boundary layer*. European Centre for Medium-Range Weather Forecasts, 2012.

S. Basu, F. Port-Agel, E. Foufoula-Georgiou, J-F. Vinuesa, and M. Pahlow. Revisiting the Local Scaling Hypothesis in Stably Stratified Atmospheric Boundary-Layer Turbulence: an Integration of Field and Laboratory Measurements with Large-Eddy Simulations. *Boundary-Layer Meteorology*, 119:473–500, 2006. ISSN 0006-8314. 10.1007/s10546-005-9036-2.

R. J. Beare, J. M. Edwards, and A. J. Lapworth. Simulation of the observed evening transition and nocturnal boundary layers: Large-eddy simulation. *Quarterly Journal of the Royal Meteorological Society*, 132(614):81–99, 2006a. ISSN 1477-870X.

R. J. Beare and M. K. Macvean. Resolution Sensitivity and Scaling of Large-Eddy Simulations of the Stable Boundary Layer. *Boundary-Layer Meteorology*, 112:257–281, 2004. ISSN 0006-8314.

R. J. Beare, M. K. Macvean, A. A. M. Holtslag, J. Cuxart, I. Esau, J-C Golaz, J. M. A., M. Khairoutdinov, B. Kosovic, D. Lewellen, T. S. Lund, J. K. Lundquist, A. Mccabe, A. F. Moene, Y. Noh, S. Raasch, and P. Sullivan. An Intercomparison of Large-Eddy Simulations of the Stable Boundary Layer. *Boundary-Layer Meteorology*, 118:247–272, 2006b. ISSN 0006-8314.

A. C. M. Beljaars and A. A. M. Holtslag. Flux Parameterization over Land Surfaces for Atmospheric Models. *Journal of Applied Meteorology*, 30(3): 327–341, Mar 1991. ISSN 0894-8763.

A. C. M. Beljaars and P. Viterbo. *Role of the Boundary Layer in a Numerical Weather Prediction Model*. Royal Netherlands Academy of Arts and Sciences, 1998.

F. C. Bosveld, P. Baas, G-J. Steeneveld, and A. A. M. Holtslag. GABLS 3 SCM intercomparison and evaluation. What did we learn? In *ECMWF Workshop on Diurnal cycles and the stable boundary layer*. European Centre for Medium-Range Weather Forecasts, 2012.

F. C. Bosveld, P. Baas, G. J. Steeneveld, A. A. M. Holtslag, W. M. Angevine, E. Bazile, E. I. F. de Bruijn, D. Deacu, J. M. Edwards, M. Ek, V. E. Larson, J. E. Pleim, M. Raschendorfer, and G. Svensson. The Third GABLS Intercomparison Case for Evaluation Studies of Boundary-layer models. Part B: Results and Process Understanding. *Boundary-Layer Meteorology*, 152:157–187, 2014a.

F. C. Bosveld, P. Baas, E. van Meijgaard, E. I. F. de Bruijn, G. J. Steeneveld, and A. A. M. Holtslag. The Third GABLS Intercomparison Case for Evaluation Studies of Boundary-layer models. Part A: Case Selection and Set-Up. *Boundary-Layer Meteorology*, 152:133–156, 2014b.

British Antarctic Survey. Time-series of sodar profiles. November 2012. URL `http://www.antarctica.ac.uk/met/psa/sodar/`.

British Atmospheric Data Centre. Mean sea-level pressure charts (ECMWF analysis). September 2012. URL `http://badc.nerc.ac.uk/view/badc.nerc.ac.uk__ATOM__dataent_ECMWF-OP`.

A. Brown, R. Beare, J. Edwards, A. Lock, S. Keogh, S. Milton, and D. Walters. Upgrades to the Boundary-Layer Scheme in the Met Office Numerical Weather Prediction Model. *Boundary-Layer Meteorology*, 128:117–132, 2008. ISSN 0006-8314. 10.1007/s10546-008-9275-0.

A. R. Brown, S. H. Derbyshire, and P. J. Mason. Large-eddy simulation of stable atmospheric boundary layers with a revised stochastic subgrid model. *Quarterly Journal of the Royal Meteorological Society*, 120(520):1485–1512, 1994. ISSN 1477-870X.

J. A. Businger and S. P. S. Arya. Height of the Mixed Layer in the Stably Stratified Planetary Boundary Layer. In F. N. Frenkiel and R. E. Munn, editors, *Turbulent Diffusion in Environmental Pollution Proceedings of a Symposium held at Charlottesville*, volume 18, Part A of *Advances in Geophysics*, pages 73 – 92. Elsevier, 1975.

J. Cuxart, A. Holtslag, R. Beare, E. Bazile, A. Beljaars, A. Cheng, L. Conangla, M. Ek, F. Freedman, R. Hamdi, A. Kerstein, H. Kitagawa, G. Lenderink, D. Lewellen, J. Mailhot, T. Mauritsen, V. Perov, G. Schayes, G-J. Steeneveld, G. Svensson, P. Taylor, W. Weng, S. Wunsch, and K-M. Xu. Single-Column Model Intercomparison for a Stably Stratified Atmospheric Boundary Layer. *Boundary-Layer Meteorology*, 118:273–303, 2006. ISSN 0006-8314. 10.1007/s10546-005-3780-1.

S. H. Derbyshire. Boundary-Layer Decoupling over Cold Surfaces as a Physical Boundary-Instability. *Boundary-Layer Meteorology*, 90:297–325, 1999. ISSN 0006-8314.

J. R. Garratt and R. A. Brost. Radiative Cooling Effects within and above the Nocturnal Boundary Layer. *Journal of the Atmospheric Sciences*, 38(12): 2730–2746, Dec 1981. ISSN 0022-4928.

M. E. B. Gray, J. Petch, S. H. Derbyshire, A. R. Brown, A. P. Lock, H. A. Swann, and P. R. A. Brown. *Version 2.3 Of The Met Office Large Eddy Model: Part II. Scientific Documentation*. Met Office (APR), 2004.

D. Handorf, T. Foken, and C. Kottmeier. The Stable Atmospheric Boundary Layer over an Antarctic Ice Sheet. *Boundary-Layer Meteorology*, 91:165–189, 1999. ISSN 0006-8314.

B. Holtslag. Preface: GEWEX Atmospheric Boundary-Layer Study (GABLS) on Stable Boundary Layers. *Boundary-Layer Meteorology*, 118:243–246, 2006. ISSN 0006-8314.

W. H. Hooke and R. M. Jones. Dissipative Waves Excited by Gravity-Wave Encounters with the Stably Stratified Planetary Boundary Layer. *Journal of the Atmospheric Sciences*, 43(19):2048–2060, Oct 1986. ISSN 0022-4928.

K Khusnutdinova. Personal communication, 2012.

J. C. King. Low-level wind profiles at an Antarctic coastal station. *Antarctic Science*, 1:169–178, 5 1989. ISSN 1365-2079.

J. C. King. Some measurements of turbulence over an Antarctic ice shelf. *Quarterly Journal of the Royal Meteorological Society*, 116(492):379–400, 1990. ISSN 1477-870X.

J. C. King and P. S. Anderson. Installation and performance of the STABLE instrumentation at Halley. *British Antarctic Survey Bulletin*, (79):65–77, 1988.

J. C. King and P. S. Anderson. Heat and water vapour fluxes and scalar roughness lengths over an Antarctic ice shelf. *Boundary-Layer Meteorology*, 69:101–121, 1994.

J. C. King, P. S. Anderson, M. C. Smith, and S. D. Mobbs. The surface energy and mass balance at Halley, Antarctica during winter. *J. Geophys. Res.*, 101 (D14):19119–19128, 1996. ISSN 0148-0227.

J. C. King, W. M. Connolley, and S. H. Derbyshire. Sensitivity of modelled Antarctic climate to surface and boundary-layer flux parametrizations. *Quarterly Journal of the Royal Meteorological Society*, 127(573):779–794, 2001. ISSN 1477-870X.

J. C. King, S. D. Mobbs, J. M. Rees, P. S. Anderson, and A. D. Culf. The Stable Antarctic boundary layer experiment at Halley Station. *Weather*, 44 (10):398–405, 1989. ISSN 1477-8696.

J. C. King and J. Turner. *Antarctic Meteorology and Climatology*. Cambridge Atmospheric and Space Science Series. Cambridge University Press, 2007. ISBN 9780521039840.

J. Kondo, O. Kanechika, and N. Yasuda. Heat and Momentum Transfers under Strong Stability in the Atmospheric Surface Layer. *Journal of the Atmospheric Sciences*, 35(6):1012–1021, Jun 1978. ISSN 0022-4928.

B. Kosovic and J. A. Curry. A Large Eddy Simulation Study of a Quasi-Steady, Stably Stratified Atmospheric Boundary Layer. *Journal of the Atmospheric Sciences*, 57(8):1052–1068, Apr 2000. ISSN 0022-4928.

C. Kottmeier. The influence of baroclinicity and stability on the wind and temperature conditions at the Georg von Neumayer Antarctic station. *Tellus*, 38A:263–276, 1986.

J-F. Louis. A parametric model of vertical eddy fluxes in the atmosphere. *Boundary-Layer Meteorology*, 17:187–202, 1979. ISSN 0006-8314.

L. Mahrt. Stratified Atmospheric Boundary Layers and Breakdown of Models. *Theoretical and Computational Fluid Dynamics*, 11:263–279, 1998. ISSN 0935-4964. 10.1007/s001620050093.

J. Malcher and H. Kraus. Low-level jet phenomena described by an integrated dynamical PBL model. *Boundary-Layer Meteorology*, 27:327–343, 1983. ISSN 0006-8314.

P. J. Mason. Large-Eddy Simulation of the Convective Atmospheric Boundary Layer. *Journal of the Atmospheric Sciences*, 46(11):1492–1516, Jun 1989. ISSN 0022-4928.

P. J. Mason and S. H. Derbyshire. Large-Eddy Simulation of the stably-stratified atmospheric boundary layer. *Boundary-Layer Meteorology*, 53: 117–162, 1990. ISSN 0006-8314.

G. L. Mellor and T. Yamada. Development of a turbulence closure model for geophysical fluid problems. *Reviews of Geophysics*, 20(4):851–875, 1982. ISSN 1944-9208.

J. W. Miles. On the stability of heterogeneous shear flows. *Journal of Fluid Mechanics*, 10, 1961.

P. Monti, H. J. S. Fernando, M. Princevac, W. C. Chan, T. A. Kowalewski, and E. R. Pardyjak. Observations of Flow and Turbulence in the Nocturnal Boundary Layer over a Slope. *Journal of the Atmospheric Sciences*, 59(17): 2513–2534, Sep 2002. ISSN 0022-4928.

W. D. Neff. *An Observational and Numerical Study of the Atmospheric Boundary Layer Overlying the East Antarctic Ice Sheet*. PhD thesis, University of Colorado, 1980.

F. T. M. Nieuwstadt. The steady-state height and resistance laws of the nocturnal boundary layer: Theory compared with Cabauw observations. *Boundary-Layer Meteorology*, 20:3–17, 1981. ISSN 0006-8314. 10.1007/BF00119920.

Y. Noh, W.G. Cheon, S.Y. Hong, and S. Raasch. Improvement of the K-profile Model for the Planetary Boundary Layer based on Large Eddy Simulation Data. *Boundary-Layer Meteorology*, 107:401–427, 2003. ISSN 0006-8314.

S. B. Pope. *Turbulent flows*. Cambridge university press, 2000.

H. H. Shin and S-Y. Hong. Intercomparison of planetary boundary-layer parametrizations in the WRF model for a single day from CASES-99. *Boundary-Layer Meteorology*, 139(2):261–281, 2011.

G. J. Steeneveld, B. J. H. van de Wiel, and A. A. M. Holtslag. Modeling the Evolution of the Atmospheric Boundary Layer Coupled to the Land Surface for Three Contrasting Nights in CASES-99. *Journal of the Atmospheric Sciences*, 63(3):920–935, Mar 2006a. ISSN 0022-4928.

GJ Steeneveld, BJH Van de Wiel, and AAM Holtslag. Modelling the arctic stable boundary layer and its coupling to the surface. *Boundary-layer meteorology*, 118(2):357–378, 2006b.

H. A. M. Sterk, G. J. Steeneveld, and A. A. M. Holtslag. The role of snow-surface coupling, radiation, and turbulent mixing in modeling a stable

boundary layer over Arctic sea ice. *Journal of Geophysical Research: Atmospheres*, 2013.

H. A. M. Sterk, G. J. Steeneveld, T. Vihma, P. S. Anderson, F. C. Bosveld, and A. A. M. Holtslag. Clear-sky stable boundary layers with low winds over snow-covered surfaces. Part 1: WRF model evaluation. *Quarterly Journal of the Royal Meteorological Society*, 141:2165–2184, 2015.

R. B. Stull. *Introduction to Boundary-Layer Meteorology*. Atmospheric Sciences Library. Kluwer Academic Pub, 1988. ISBN 9789027727695.

G. Svensson, A. Holtslag, V. Kumar, T. Mauritsen, G. Steeneveld, W. Angevine, E. Bazile, A. Beljaars, E. de Bruijn, A. Cheng, L. Conangla, J. Cuxart, M. Ek, M. Falk, F. Freedman, H. Kitagawa, V. Larson, A. Lock, J. Mailhot, V. Masson, S. Park, J. Pleim, S. Sderberg, W. Weng, and M. Zampieri. Evaluation of the Diurnal Cycle in the Atmospheric Boundary Layer Over Land as Represented by a Variety of Single-Column Models: The Second GABLS Experiment. *Boundary-Layer Meteorology*, 140:177–206, 2011. ISSN 0006-8314.

B. J. H. Van de Wiel, R. J. Ronda, A. F. Moene, H. A. R. De Bruin, and A. A. M. Holtslag. Intermittent Turbulence and Oscillations in the Stable Boundary Layer over Land. Part I: A Bulk Model. *Journal of the Atmospheric Sciences*, 59(5):942–958, Mar 2002. ISSN 0022-4928.

W. Weng and P. A. Taylor. On modelling the 1-D atmospheric boundary layer. *Boundary-Layer Meteorology*, 107:371–400, 2003.

S. S. Zilitinkevich. On the determination of the height of the Ekman boundary layer. *Boundary-Layer Meteorology*, 3:141–145, 1972. ISSN 0006-8314. 10.1007/BF02033914.

